Russian Geology and Geophysics © 2020, V.S. Sobolev IGM, Siberian Branch of the RAS
Vol. 61, No. 2, pp. 234–240, 2020 *DOI:10.15372/RGG2019097* *Geologiya i Geofizika*

Recording the Vertical Component of the Electric Field in Magnetotelluric Sounding

V.V. Plotkin[a, ✉], V.S. Mogilatov[a,b, †]

[a] *Trofimuk Institute of Petroleum Geology and Geophysics, Siberian Branch of the Russian Academy of Sciences, pr. Akademika Koptyuga 3, Novosibirsk, 630090, Russia*

[b] *Novosibirsk State University, ul. Pirogova 1, Novosibirsk, 630090, Russia*

Received 6 April 2018; received in revised form 26 July 2018; accepted 21 March 2019

Abstract—Magnetotelluric sounding (MTS) usually records variations in five components of the electromagnetic field. Interpretation of distorted MT responses of an inhomogeneous earth may be problematic. The problem can be solved by recording additionally the vertical component *Ez* of the electric field in order to improve the quality of inversion and to gain more information. Currently *Ez* variations are estimated by measuring voltage on a vertical line immersed in water. The land measurements of this kind require special drilling or using the existing boreholes, which is not always feasible. Otherwise, a circular electric dipole (CED) can be used as a receiver to record the electric field behavior along the vertical component. Its applicability to MT soundings is analyzed in this paper.

Keywords: magnetotelluric sounding, electrical conductivity, circular electric dipole, distortion of apparent resistivity curves, vertical component of electric field

INTRODUCTION

Magnetotelluric (MT) surveys commonly yield five components of the electromagnetic field proceeding from the Tikhonov-Cagniard model that simulates responses of a laterally uniform layered earth to a vertical incident plane EM wave. The classical approach addresses transfer functions that relate the horizontal components of the electric ($E_{x,y}$) and magnetic ($H_{x,y}$) fields, while the fifth component, that of vertical magnetic field (H_z), represents the departure from the reference model.

The vertical component of the electric field (E_z) zeroes at the earth-air interface, because the electrical conductivity of air is very low ($\sigma_a \sim 10^{-14}$ S/m) and the transverse current is continuous. Unlike this ideal case, the E_z component of real responses is zero only at the very interface but is nonzero and decaying gradually in the near-surface skin layer. Furthermore, E_z may be nonzero at the earth-air interface as well if the skin layer is anisotropic and the transverse current direction departs from this component. In the field practice, the E_z component (like the $E_{x,y}$ one) is determined by measuring voltage on a finite-length line, which is presumably nonzero and dependent on the line length.

To improve the inversion quality, it is pertinent to compare the E_z values retrieved by 3D inversion for each model with the measured data. Distorted MT responses of an inhomogeneous earth may be problematic to interpret. Neglect of possible distortions in the presence of shallow lateral inhomogeneities may lead to errors in apparent resistivity and depth of conductors (Wannamaker et al., 1984; Ingham, 1988).

Soundings in such areas are run with unconventional MT configurations and the data are processed with specially designed algorithms. Possible solutions are to average spatially the horizontal components of the electric field recorded with long lines (Torres-Verdin and Bostick, 1992) or to record the vertical component E_z of the electric field. The E_z data can be acquired with a so-called circular electric dipole (CED) placed on the ground surface, and its applicability is analyzed below.

The circular electric dipole was first used as a radiated transmitter in controlled-source transient electromagnetic (TEM) surveys (Mogilatov, 1982). See Fig. 1 for an ideal model of eddy currents and a real transmitter configuration. CED transmitters have been employed successfully in TEM surveys (Mogilatov, 2014) and are advantageous by exciting the TM mode that has only the vertical component of the electric field in a layered earth. Since the magnetic field of the TM mode is zero in nonconducting air, the surface data lack the direct field contribution while all variations of the magnetic field represent deviations from the layered earth model.

The circular electric dipole consists of eight radiated long lines (Fig. 1). Its feature of exciting the TM mode with the

† Deceased.
✉ Corresponding author.
E-mail address: PlotkinVV@ipgg.sbras.ru (V.V. Plotkin)

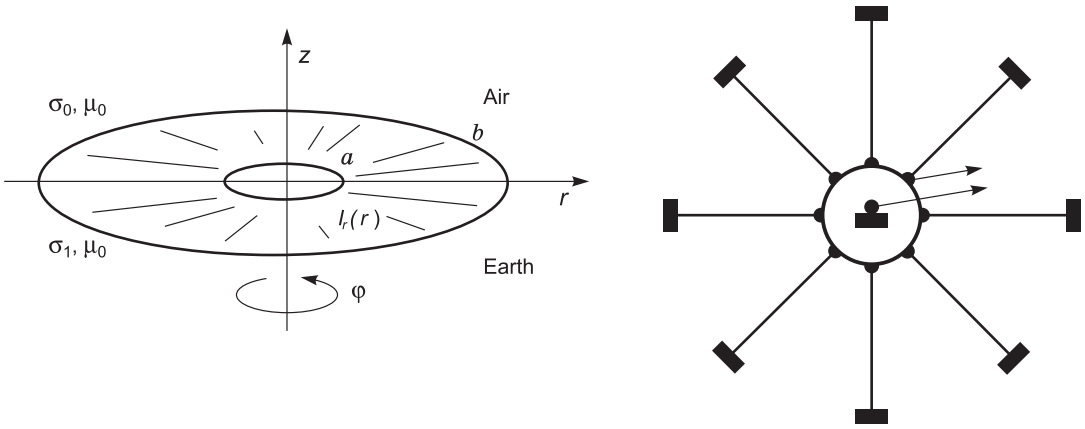

Fig. 1. Circular electric dipole: an ideal model and a real radiated configuration

vertical electric field component (E_z) makes it suitable as a receiver for recording E_z variations beneath MT stations. In the current survey practice, these variations are measured as voltage of a vertical line immersed in water (e.g., Shneer et al., 2007; Moroz et al., 2008). On the land, this approach requires additional drilling or using existing boreholes, which may be unfeasible. In this respect, search for new ways of recording E_z is of special interest. New experimental evidence on E_z variations can make an important contribution to many aspects of geophysics. We analyze the applicability of CED to record the behavior of the E_z component in MT sounding.

3D ANALYTICAL MODEL OF MT SOUNDING

Let a conducing thin sheet with the total longitudinal conductance $\Sigma(x, y)$ be located at the depth z' in a homogeneous earth. The conductivity of the earth can be presented as the sum $\sigma + \sigma'(x, y, z)$ where $\sigma'(x, y, z) = \Sigma(x, y)\,\delta(z - z')$, and $\delta(z)$ is the delta function. The method of perturbations works in this case.

In the zero-approximation, for vertical plane-wave incidence, $\mathbf{E}^{(0)} = \mathbf{E}_0 \exp(-k_0 z)$, $k_0^2 = i\omega\mu_0\sigma$ (OZ axis is directed depthward). The first-approximation field $\mathbf{E}^{(1)}$ (Plotkin, 2017) is

$$\Delta E^{(1)}_{x,y} - k_0^2 E^{(1)}_{x,y} = F_{x,y}\delta(z - z'),$$
$$F_x = E^{(0)}_x(z')\left(i\omega\mu_0\Sigma - \frac{1}{\sigma}\frac{\partial^2\Sigma}{\partial x^2}\right) - E^{(0)}_y(z')\frac{1}{\sigma}\frac{\partial^2\Sigma}{\partial x\partial y}, \qquad (1)$$
$$F_y = -E^{(0)}_x(z')\frac{1}{\sigma}\frac{\partial^2\Sigma}{\partial x\partial y} + E^{(0)}_y(z')\left(i\omega\mu_0\Sigma - \frac{1}{\sigma}\frac{\partial^2\Sigma}{\partial y^2}\right).$$

The Fourier expansion $\sim\exp\left(i\omega t + ik_x x + ik_y y\right)$ of the fields $E^{(1)}_{x,y}$ and $\Sigma(x, y)$ in (1) and integrating along OZ in the vicinity of the thin sheet leads to

$$\left.\frac{de^{(1)}_{x,y}}{dz}\right|_{z'+0} - \left.\frac{de^{(1)}_{x,y}}{dz}\right|_{z'-0} = f_{x,y},$$
$$f_x = E^{(0)}_x(z')\left(i\omega\mu_0 + \frac{k_x^2}{\sigma}\right)\Sigma_k + E^{(0)}_y(z')\frac{k_x k_y}{\sigma}\Sigma_k, \qquad (2)$$
$$f_y = E^{(0)}_x(z')\frac{k_x k_y}{\sigma}\Sigma_k + E^{(0)}_y(z')\left(i\omega\mu_0 + \frac{k_y^2}{\sigma}\right)\Sigma_k,$$

where $e^{(1)}_{x,y}(z)$, $f_{x,y}$, Σ_k are the amplitudes of the Fourier harmonics of the respective values.

The solution to (1) for the $e^{(1)}_{x,y,z}(z)$ components is found as below, taking into account that $\mathrm{div}\mathbf{E}^{(1)} = 0$ outside the conducting thin sheet; the air conductivity is σ_a; and $z = 0$ is the earth surface:

$$e^{(1)}_{x,y} = A_{x,y}e^{k_a z},\ e^{(1)}_z = -(ik_x A_x + ik_y A_y)\frac{e^{k_a z}}{k_a},\quad z < 0,$$
$$e^{(1)}_{x,y} = C^+_{x,y}e^{k(z-z')} + C^-_{x,y}e^{-k(z-z')},\quad 0 < z < z',$$
$$e^{(1)}_z = -(ik_x C^+_x + ik_y C^+_y)\frac{e^{k(z-z')}}{k} + \qquad (3)$$
$$(ik_x C^-_x + ik_y C^-_y)\frac{e^{-k(z-z')}}{k},$$
$$e^{(1)}_{x,y} = D_{x,y}e^{-k(z-z')},\ e^{(1)}_z =$$
$$(ik_x D_x + ik_y D_y)\frac{e^{-k(z-z')}}{k},\quad z' < z,$$
$$k_a^2 = \bar{k}^2 + i\omega\mu_0\sigma_a,\ k^2 = \bar{k}^2 + i\omega\mu_0\sigma,\ \bar{k} = \sqrt{k_x^2 + k_y^2},$$

Eight constants in (3) are found using the boundary conditions: linking (2) and continuity for the components $e^{(1)}_{x,y}$

at $z = z'$ and continuity for the components of the electric ($e^{(1)}_{x,y}$) and magnetic ($h^{(1)}_{x,y}$) fields at $z = 0$ (earth-air interface). The sought constants and field components are determined by solving the system of equations (choice of +/- superscripts corresponds to the first subscripts):

$$C^{+}_{x,y} = -\frac{f_{x,y}}{2k},\ C^{-}_{x,y} = -e^{-2kz'}\left[\frac{f_{y,x}}{2k}R_1R_2 + \frac{f_{x,y}}{2k}R_1R^{\pm}\right],$$

$$D_{x,y} = -\frac{f_{y,x}}{2k}R_1R_2e^{-2kz'} - \frac{f_{x,y}}{2k}\left[1 + R_1R^{\pm}e^{-2kz'}\right],$$

$$e_{x,y}\Big|_{z=0} = A_{x,y} = -\frac{f_{x,y}}{2k}e^{-kz'}\left[1 + R_1R^{\pm}\right] - \frac{f_{y,x}}{2k}R_1R_2e^{-kz'},$$

$$e_z = \frac{ik_xf_x + ik_yf_y}{2k^2}\left[e^{kz} - R_1R_3e^{-kz}\right]e^{-kz'},\ \ 0 < z < z', \tag{4}$$

$$e_z = -\frac{ik_xf_x + ik_yf_y}{2k^2}\left[e^{kz'} + R_1R_3e^{-kz'}\right]e^{-kz},\ \ z' < z,$$

$$R_1 = \frac{k - k_a}{k + k_a},\ R_2 = \frac{2k_xk_y}{kk_a - \bar{k}^2},\ R_3 = \frac{kk_a + \bar{k}^2}{kk_a - \bar{k}^2},$$

$$R^{\pm} = \frac{kk_a \pm k_x^2 \mp k_y^2}{kk_a - \bar{k}^2}.$$

RECORDING THE E_z COMPONENT WITH A CED

The equations for voltage along a vertical line in the subsurface and for that of an ideal CED are:

$$U_z(x,y) = \iint dk_xdk_y\ e^{ik_xx + ik_yy}\int_0^{\infty} e_z(k_x,k_y,z)dz,$$

$$U_{\mathrm{CED}}(x,y) = -\iint dk_xdk_y\ e^{ik_xx + ik_yy}e^{TM}(k_x,k_y,0). \tag{5}$$

The equation for U_{CED} in (5) includes the potential e^{TM} of the TM mode electric field ($e^{\mathrm{TM}} \to 0$ in infinity) since the vertical component e_z is nonzero only in this mode (Plotkin, 2014):

$$e_x = ik_xe^{\mathrm{TM}} + ik_ye^{\mathrm{TE}},\ e_y = ik_ye^{\mathrm{TM}} - ik_xe^{\mathrm{TE}},$$

$$e^{\mathrm{TM}} = -\frac{ik_xe_x + ik_ye_y}{k_x^2 + k_y^2},\ \ e^{\mathrm{TE}} = -\frac{ik_ye_x - ik_xe_y}{k_x^2 + k_y^2}, \tag{6}$$

$$e_z = \frac{k_x^2 + k_y^2}{k^2}\frac{de^{\mathrm{TM}}}{dz},\ \ h_z = -\frac{1}{i\omega\mu_0}(k_x^2 + k_y^2)e^{\mathrm{TE}},$$

where e^{TE} is the potential of the TE mode. Integration along z with (4) for U_z in (5), taking into account the equations for e^{TM} and e^{TE} in (6), leads to

$$U_z(x,y) = -\iint dk_xdk_y\ e^{ik_xx + ik_yy}\frac{ik_xf_x + ik_yf_y}{k^2(k + k_a)}\frac{k_a}{k}e^{-kz'},$$

$$U_{\mathrm{CED}}(x,y) = -\iint dk_xdk_y\ e^{ik_xx + ik_yy}\frac{ik_xf_x + ik_yf_y}{(k_x^2 + k_y^2)(k + k_a)}\frac{k_a}{k}e^{-kz'}, \tag{7}$$

$$H_z(x,y) = -\frac{1}{i\omega\mu_0}\iint dk_xdk_y\ e^{ik_xx + ik_yy}\frac{ik_yf_x - ik_xf_y}{k + k_a}e^{-kz'}.$$

As it follows from (6) and (7), the e^{TE} refers to the vertical component of the magnetic field H_z, while the integrand functions for U_z and U_{CED}, which coincide at $(k_x^2 + k_y^2) >> \omega\mu_0\sigma$, refer to the TM mode. The condition $(k_x^2 + k_y^2) >> \omega\mu_0\sigma$ fulfills at low frequencies (long periods), when lateral inhomogeneities are much smaller than the skin depth. This case corresponds to galvanic distortion of MT responses in an electrostatic field that arises in a thin sheet with such features (Plotkin, 2014). Therefore, the use of CED in this case can provide additional constraints on frequency dependence of the voltage U_z in a virtual borehole.

AXISYMMETRICAL LATERAL INHOMOGENEITIES

The voltage U_z and U_{CED} can be presented in cylindrical coordinates, with regard to (2) for $f_{x,y}$,:

$$U_z(r,\alpha) = -\int_0^{\infty}\bar{k}d\bar{k}\int_0^{2\pi}d\varphi\ e^{i\bar{k}r\cos(\varphi-\alpha)}\frac{i\bar{k}E_{0r}}{(k + k_a)}\frac{k_a}{k}\frac{\Sigma_k(\bar{k},\varphi)}{\sigma}e^{-(k_0+k)z'},$$

$$U_{\mathrm{CED}}(r,\alpha) = -\int_0^{\infty}\bar{k}d\bar{k}\int_0^{2\pi}d\varphi\ e^{i\bar{k}r\cos(\varphi-\alpha)}\frac{kk_a}{\bar{k}^2}\frac{i\bar{k}E_{0r}}{(k + k_a)}\frac{\Sigma_k(\bar{k},\varphi)}{\sigma}e^{-(k_0+k)z'}, \tag{8}$$

where

$$k_x = \bar{k}\cos\varphi,\ k_y = \bar{k}\sin\varphi,\ \bar{k} = \sqrt{k_x^2 + k_y^2},$$

$$x = r\cos\alpha,\ y = r\sin\alpha,\ r = \sqrt{x^2 + y^2},$$

$$k = \sqrt{\bar{k}^2 + k_0^2}\ ,$$

$$k_a = \sqrt{\bar{k}^2 + i\omega\mu_0\sigma_a},\ E_{0r}(\varphi) = E_{0x}\cos\varphi + E_{0y}\sin\varphi.$$

For clarity, it is pertinent to focus on axisymmetrical lateral inhomogeneities when $\Sigma(x,y) = \Sigma(r)$, $\Sigma_k(\bar{k},\varphi) = \Sigma_k(\bar{k})$:

$$\Sigma_k(\bar{k}) = \frac{1}{(2\pi)^2}\int_0^{\infty}\Sigma(r)\ rdr\int_0^{2\pi}e^{i\bar{k}r\cos(\varphi-\alpha)}d\varphi = \frac{1}{2\pi}\int_0^{\infty}\Sigma(r)J_0(\bar{k}r)rdr, \tag{9}$$

where $J_0(\bar{k}r)$ is the Bessel function. Taking into account (9), the integrals over the angle φ in (8) are found explicitly. Then, the voltage equations become

$$U_z(r,\alpha) = 2\pi E_{0r}\int_0^\infty \frac{\Sigma_k(\bar{k})}{\sigma}\frac{\bar{k}J_1(\bar{k}r)}{(k+k_a)}\frac{k_a}{k}e^{-(k_0+k)z'}\bar{k}d\bar{k},$$
$$U_{\mathrm{CED}}(r,\alpha) = 2\pi E_{0r}\int_0^\infty \frac{\Sigma_k(\bar{k})}{\sigma}\frac{\bar{k}J_1(\bar{k}r)}{(k+k_a)}\frac{kk_a}{\bar{k}^2}e^{-(k_0+k)z'}\bar{k}d\bar{k}. \quad (10)$$

In (10), $E_{0r}(\alpha) = E_{0x}\cos\alpha + E_{0y}\sin\alpha$ is the radial component of the primary field and $J_1(\bar{k}r)$ is the Bessel function. Let a solitary inhomogeneity be specified as $\Sigma(r) = \Sigma_0$ at $r < r_0$, and $\Sigma(r) = 0$ at $r > r_0$. For further simplification, assume that $r_0 \to 0, \Sigma_0 \to \infty$; consequently, $r_0^2\Sigma_0 = \mathrm{const}$ and $\Sigma_k = \dfrac{r_0^2\Sigma_0}{4\pi}$ (equivalent of a delta function). Then,

$$U_z(r,\alpha) = E_{0r}e^{-k_0z'}\frac{r_0^2\Sigma_0}{2\sigma}$$
$$\int_0^\infty \frac{\xi^2 J_1(\xi r)e^{-\sqrt{\xi^2+k_0^2}z'}}{\sqrt{\xi^2+k_0^2}+\sqrt{\xi^2+k_0^2\sigma_a/\sigma}}\frac{\sqrt{\xi^2+k_0^2\sigma_a/\sigma}}{\sqrt{\xi^2+k_0^2}}d\xi,$$
$$U_{\mathrm{CED}}(r,\alpha) = E_{0r}e^{-k_0z'}\times$$
$$\frac{r_0^2\Sigma_0}{2\sigma}\int_0^\infty \frac{\sqrt{\xi^2+k_0^2}\sqrt{\xi^2+k_0^2\sigma_a/\sigma}}{\sqrt{\xi^2+k_0^2}+\sqrt{\xi^2+k_0^2\sigma_a/\sigma}}J_1(\xi r)e^{-\sqrt{\xi^2+k_0^2}z'}d\xi, \quad (11)$$

$$H_z(r,\alpha) = E_{0\alpha}e^{-k_0z'}\frac{r_0^2\Sigma_0}{2}\int_0^\infty \frac{\xi^2 J_1(\xi r)e^{-\sqrt{\xi^2+k_0^2}z'}}{\sqrt{\xi^2+k_0^2}+\sqrt{\xi^2+k_0^2\sigma_a/\sigma}}d\xi.$$

$E_{0\alpha} = E_{0x}\sin\alpha - E_{0y}\cos\alpha$ is the azimuthal component of the primary field.

At low frequencies, $k_0 \to 0$, all integrals in (11) coincide and can be obtained in the explicit form. In this case, charge polarization at the inhomogeneity produces a subsurface electrostatic field, with its geometry the same as that of the CED field at the inhomogeneity center at the depth z′ and its axis along the primary field.

$$E_r^{(1)}(r,\alpha) = E_{0r}e^{-k_0z'}\frac{r_0^2\Sigma_0}{4\sigma}\left[\frac{3r^2}{(r^2+z'^2)^{5/2}} - \frac{1}{(r^2+z'^2)^{3/2}}\right],$$
$$E_\alpha^{(1)}(r,\alpha) = E_{0\alpha}e^{-k_0z'}\frac{r_0^2\Sigma_0}{4\sigma}\frac{1}{(r^2+z'^2)^{3/2}}, \quad (12)$$
$$U_z(r,\alpha) = U_{\mathrm{CED}}(r,\alpha) = E_{0r}e^{-k_0z'}\frac{r_0^2\Sigma_0}{2\sigma}\frac{r}{(r^2+z'^2)^{3/2}}.$$

$$H_z(r,\alpha) = E_{0\alpha}e^{-k_0z'}\frac{r_0^2\Sigma_0}{2}\frac{r}{(r^2+z'^2)^{3/2}}.$$

Equation (12) includes the surface components of the TM mode electric field while the respective components in the TE mode are low: $\sim k_0r_0^2$. All functions in (12) are proportional to $r_0^2\Sigma_0$ which can be called bulk conductivity of a lateral inhomogeneity (by analogy with the total longitudinal conductance of the thin sheet Σ_0). The component H_z of the TE mode magnetic field in (12) is frequency independent (except for attenuation of the primary wave $e^{-k_0z'}$).

As the frequency increases, at $k_0^2 = i\omega\mu_0\sigma$, the e^{TE} amplitude and the voltage of the TE mode increase as well:

$$U^{\mathrm{TE}}(r,\alpha) =$$
$$-k_0^2E_{0\alpha}e^{-k_0z'}\frac{r_0^2\Sigma_0}{2\sigma}\int_0^\infty \frac{J_1(\xi r)e^{-\sqrt{\xi^2+k_0^2}z'}}{\sqrt{\xi^2+k_0^2}+\sqrt{\xi^2+k_0^2\sigma_a/\sigma}}d\xi. \quad (13)$$

Furthermore, U_z becomes different from U_{CED} in (11) as $k_0^2 = i\omega\mu_0\sigma$ increases, and the difference is associated with the contribution of small $\bar{k} \le k_0$ into the integrals in (11). Small $\bar{k} << k_0$ correspond to the case of a strong skin effect when the characteristic size of lateral inhomogeneities far exceeds the skin depth. In fact, it means the lack of lateral inhomogeneity and leads to low values of U_z. Since $J_1(\bar{k}r) \to 0$ at low $\bar{k}r$, the difference between U_z and U_{CED} can be inferred to appear only far from the axisymmetrical inhomogeneity at distances exceeding the skin depth $r > 1/|k_0|$. Figure 2 provides an example of curves that characterize the k_0-dependent increase of the $U_z(r) - U_{\mathrm{CED}}(r)$

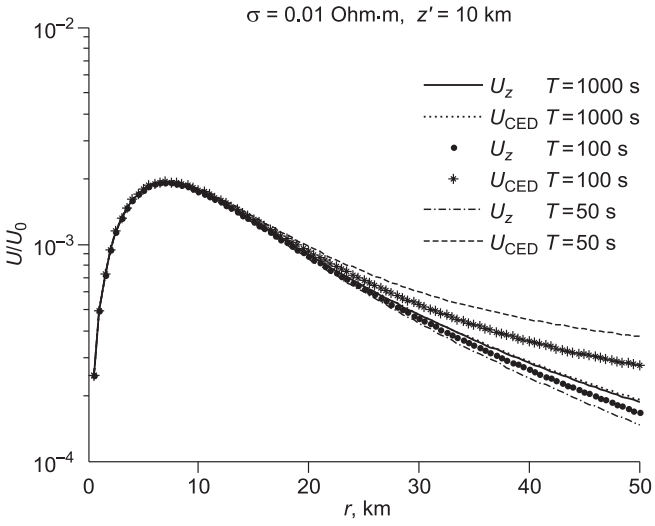

Fig. 2. $U_z(r)$ and $U_{\mathrm{CED}}(r)$ at different frequencies (in relative units, $U_0 = E_{0r}e^{-k_0z'}\dfrac{r_0^2\Sigma_0}{2\sigma}$).

difference (in relative units, $U_0 = E_{0r}e^{-k_0 z'}\frac{r_0^2\Sigma_0}{2\sigma}$). This difference becomes notable only far from the inhomogeneity center, where both voltage values begin to decrease.

USE OF CED FOR MTS: A NUMERICAL MODEL

The consideration above has concerned the voltage recorded by an ideal CED consisting of continuous infinite-length radial lines. However, the number and length of lines in real surveys are limited: a CED transmitter (Mogilatov, 2014) can have eight lines distributed uniformly according to azimuth. The CED radius is an important parameter that controls the relative magnitudes of U_z and U_{CED}. Its effect in a CED used as a receiver in MTS can be analyzed by simulation.

The modeling below is based on the Trefftz method (Plotkin and Gubin, 2015) and accounts for distortions in MT responses of an earth with a 3D inhomogeneity. The model consists of seven layers with the resistivities 25, 50, 100, 1000, 10, 1000, and 1 Ohm·m (from top to bottom) of the respective thicknesses 0.1, 0.1, 0.1, 15, 10, 45, and 15 km, which lie on a 100 Ohm·m base (Fig. 3*a*). The resistivity depth profile includes two conductors in the crust at depths of 15–25 km and in the mantle at 70–85 km. Three 0.1 km thick upper layers can be used to simulate perturbations of MT responses, specifically, the effect of a single inhomogeneity feature in the second upper layer (Fig. 3*b*).

The model MT survey is applied to a 30 × 30 km area, with a CED receiver in the center (straight radial lines in Fig. 3*b*). Each of the seven layers in the model is presented by 49 identical homogeneous blocks with their thickness equal to the layer thickness and 4.29 × 4.29 km sizes in the horizontal plane (seven blocks along each horizontal coordinate axis). Maxwell's equations solved for each block describe shear waves propagating counterwise along each coordinate axis: 12 waves (with regard to polarization). The unknown amplitudes of these waves are found by solving the general system of equations derived proceeding from the linking conditions for shear field components at all faces of the blocks, as well as from boundary conditions. The amplitude estimates are used to calculate all components of the electromagnetic field at the centers of the blocks and on the surface. Then U_z and U_{CED} are determined as integrals over the longitudinal components of the electric field along the vertical and radial receiver lines. The impedance tensor components are calculated separately for two independent polarizations of a plane wave of normal incidence. The voltage values U_z and U_{CED} are also found for each of two independent polarizations of the primary wave. Their difference is nonzero at the given CED configuration with respect to the inhomogeneity and corresponds to the chosen polarization of the magnetic field induced by a primary wave along *OY*.

The apparent resistivity curves for the site center (Fig. 4), at two resistivity values of the inhomogeneity in the second upper layer (Fig. 3*b*), show notable galvanic distortions. Namely, the ρ_{xy} and ρ_{yx} curves are shifted along the *y* axis

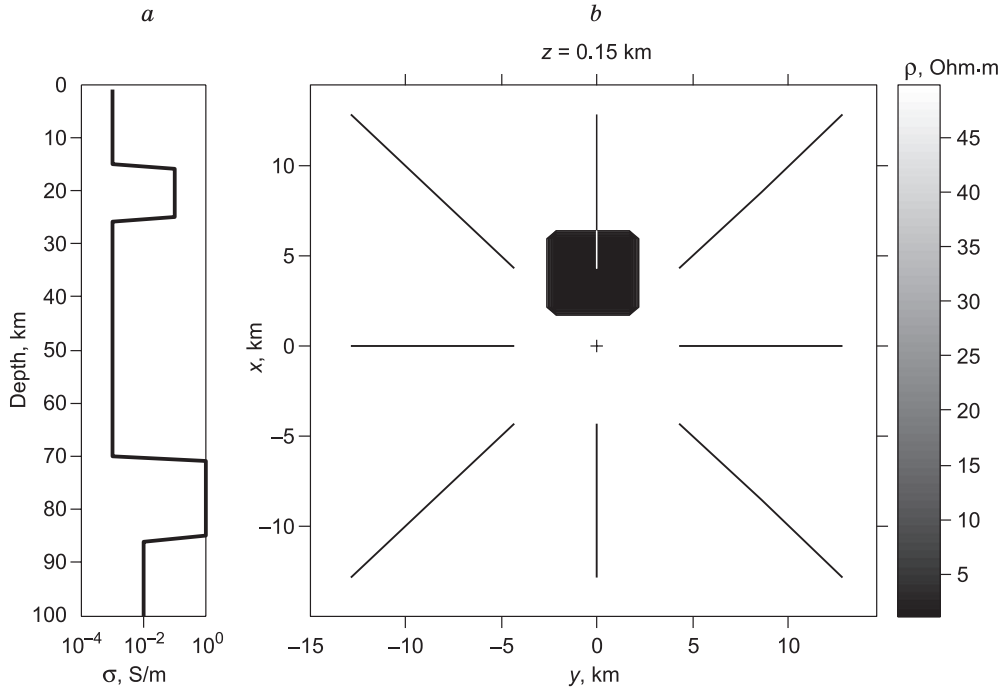

Fig. 3. A 3D earth model. *a*, Normal resistivity-depth profile; *b*, laterally inhomogeneous near-surface layer: horizontal plane. Radiated CED lines on the surface; cross marks the center.

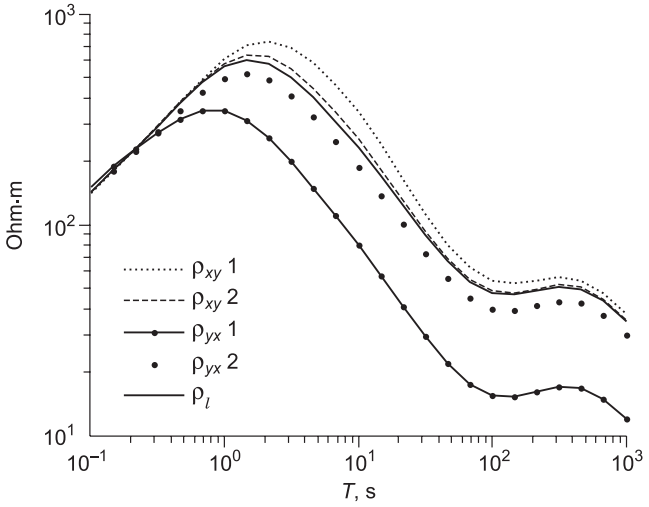

Fig. 4. Apparent resistivity curves ρ_{xy} and ρ_{yx} (center) for two resistivity values ρ_n of the inhomogeneity. 1, ρ_n =1 Ohm·m; 2, ρ_n =10 Ohm·m, ρ_l is the background resistivity.

relative to the normal ρ_l curve at long periods: the lower the resistivity of the inhomogeneity the greater the shift.

Figure 5 shows period-dependent behavior of U_z and U_{CED} at the center of the site (cross in Fig. 3*b*), for different parameters of the lateral inhomogeneity: the resistivity ρ_n, the bulk conductivity $r_0^2\Sigma_0$, and the distance from the CED center r_n. At variable resistivity (conductivity) of the inhomogeneity, all other parameters being equal (Fig. 5*a*), the U_z and U_{CED} values are proportional to the resistivity departure from the background.

Since a real CED differs from an ideal one in number and length of radial lines, the U_z and U_{CED} curves become shifted relative to one another along the y axis. The curves of Fig. 5*a* are corrected for this shift at long periods by multiplying all values along the U_{CED} curve by a factor of 3.5. Note that the factor is the same for different resistivities of the inhomogeneity, while all other conditions are equal. A small shift persists at short periods, which confirms the above inference for an ideal CED.

At shorter distances from the inhomogeneity center, with invariable bulk conductivity $r_0^2\Sigma_0$, the curves U_z and U_{CED} coincide over a larger range of long periods (Fig. 5*b*). The curves for case 3 were obtained for a 10 × 10 km site, the inhomogeneity resistivity ρ_n = 1.1 Ohm·m, and equal other conditions. The normalization factor for U_{CED} curves in case 3 was 1.12.

CONCLUSIONS

Magnetotelluric sounding commonly records five components of the electromagnetic field. However, the interpretation of real distorted MT responses of an inhomogeneous earth may be problematic. It is suggested to record additionally variations of the MT field along the vertical electric component acquired by a circular electric dipole (CED), in order to improve the quality of inversion and gain more information.

The reported analytical model shows that the voltage U_{CED} recorded by an ideal CED perfectly agrees with that recorded by a vertical line (U_z) if lateral inhomogeneities are much smaller than the skin depth at long periods (low frequencies). This voltage behavior corresponds to the case of galvanic distortions of MT responses in an electrostatic field produced by lateral inhomogeneities. CED additionally records period-dependent U_z variations along a vertical line in a virtual borehole.

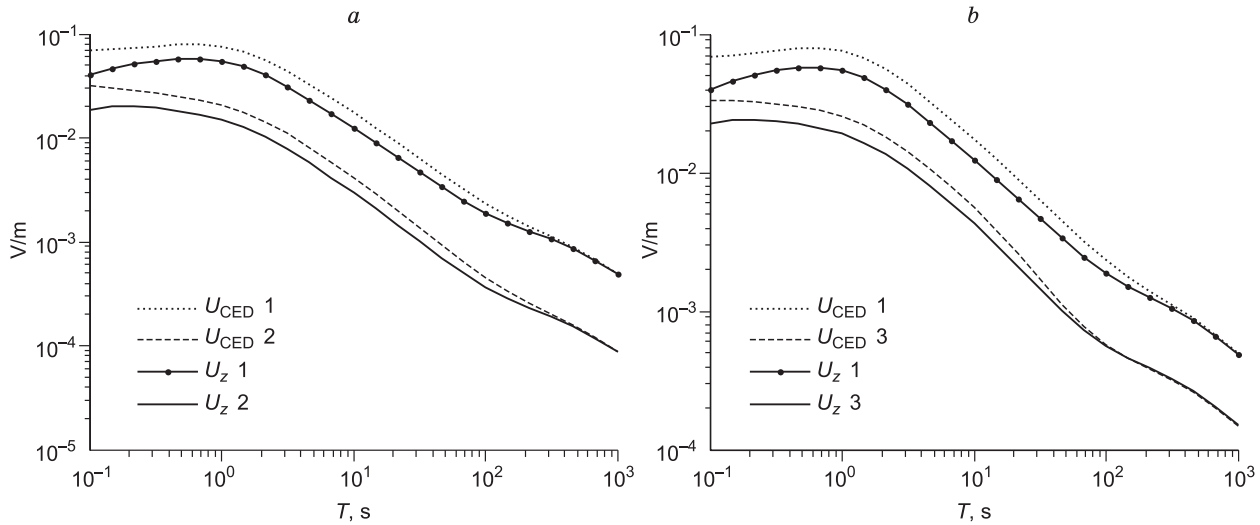

Fig. 5. Period dependence of voltage for a vertical line in the center (U_z) and total voltage over all radiated CED lines (U_{CED}), at different parameters of lateral inhomogeneity: bulk conductivity $r_0^2\Sigma_0$ and distance r_n to the center of CED. *a:* 1, ρ_n = 1 Ohm·m, r_n = 4.29 km, $r_0^2\Sigma_0 = 1.84 \times 10^9$ S·m^2; 2, ρ_n =10 Ohm·m, r_n = 4.29 km, $r_0^2\Sigma_0 = 1.84 \times 10^8$ S·m^2. *b:* 1, ρ_n =1 Ohm·m, r_n = 4.29 km, $r_0^2\Sigma_0 = 1.84 \times 10^9$ S·m^2; 3, ρ_n =1.1 Ohm·m, r_n = 1.43 km, $r_0^2\Sigma_0 = 1.84 \times 10^9$ S·m^2.

The use of a CED receiver has been modeled for the case of a solitary inhomogeneity in a layered earth. The controlled difference of a real CED from an ideal one (in number and length of radial lines) produces a shift along the y axis between the U_z and U_{CED} curves. The shift does not depend on the inhomogeneity resistivity, other conditions being equal. After the respective shift correction at long periods, minor difference between U_z and U_{CED} still remains at short periods.

Thus, the voltage measured with CED for an electric field excited by a normal incident plane wave in a 3D earth is equivalent to that of a long vertical line at the CED center. In practice it means that voltage data can be collected along a vertical line without drilling.

We appreciate interest to our study and useful advice by E.V. Pospeeva and V.A. Pospeev.

The work was supported by grant 18-17-00095 from the Russian Science Foundation.

REFERENCES

Ingham, M.R., 1988. The use of invariant impedances in magnetotelluric interpretation. Geophys. J. Int. 92 (1), 165–169.

Mogilatov, V.S., 1982. A Method for Resistivity Survey. Patent RF No. 1062631. Published 23.12.1983 [in Russian]. Bull. No. 47.

Mogilatov, V.S., 2014. Induction Resistivity Survey [in Russian]. NGU. Novosibirsk.

Moroz, Yu.F., Moroz, T.A., Buglova, S.G., 2008. Vertical and horizontal components of the lake Baikal electrotelluric field and their relation to the electric conductivity. Izvestiya, Phys. Solid Earth 44, 239–248.

Plotkin, V.V., 2014. Effects of near-surface inhomogeneities on MT responses: An analytical model. Russian Geology and Geophysics (Geologiya i Geofizika) 55 (4), 515–521 (660–668).

Plotkin, V.V., 2017. Fast computation of MT curves for a horizontally layered earth with laterally inhomogeneous conductivity perturbations. Russian Geology and Geophysics (Geologiya i Geofizika) 58 (11), 1441–1451 (1812–1827).

Plotkin, V.V., Gubin, D.I., 2015. Accounting for near-surface inhomogeneities over a horizontally layered section in magnetotelluric sounding. Russian Geology and Geophysics (Geologiya i Geofizika) 56 (7), 1083–1090 (1381–1390).

Shneer, V.S., Gaidash, S.P., Trofimov, I.L., Korotaev, S.M., Kuznetsova, T.V., Tsirulnic, L.B., Panfilov, A.I., Budnev, N.M., Mirgazov, R.R., 2007. Long-term observations of the electric field vertical component in Lake Baikal (preliminary results). Izvestiya, Phys. Solid Earth 43, 331–335.

Torres-Verdin, C., Bostick, F.X., 1992. Principles of spatial surface electric field filtering in magnetotellurics: electromagnetic array profiling (EMAP). Geophysics 57 (4), 587–602.

Wannamaker, P.E., Hohmann, G.W., Ward, S.H., 1984. Magnetotelluric responses of three-dimensional bodies in layered Earths. Geophysics 49 (9), 1517–1533.

Editorial responsibility: M.I. Epov